Nonlinearity management: a route to high-energy soliton fiber lasers

Fatih Ö. Ilday and Frank W. Wise

Department of Applied Physics, Cornell University, Ithaca, New York 14853

Received May 29, 2001; revised manuscript received August 27, 2001

We propose the use of self-defocusing nonlinearities to control nonlinear phase shifts in soliton fiber lasers. By analogy to dispersion management, we refer to this scheme as nonlinearity management. First we describe a map that can be regarded as a combination of nonlinearity management and dispersion management. The map is designed to support solitons in two segments of alternating sign of nonlinearity and dispersion. Analytical and numerical calculations demonstrate that this map can be essentially free of spectral-sideband generation. Suppressing the spectral sidebands should make possible pulse energies 100 times greater than those of existing soliton fiber lasers. We also discuss the less than ideal case of direct reduction of average nonlinearity by use of self-defocusing nonlinearity segments without optimizing dispersion. The second scheme has the advantage of easier implementation. Practical implementations with existing materials are discussed. © 2002 Optical Society of America

OCIS codes: 320.7090, 320.5540, 060.5530.

1. INTRODUCTION

Fiber lasers have emerged as attractive alternatives to solid-state lasers for generation of femtosecond pulses at near-infrared wavelengths. Fiber lasers possess considerable advantages compared with solid state lasers, most notably, simplicity of operation. Their high stability compared with solid state lasers, combined with their compact size, offers the possibility of widespread application. The drawbacks of fiber lasers are their insufficient environmental stability for use outside the research laboratory and their lack of high pulse energies directly from an oscillator. The obstacles to generation of higher-energy and shorter pulses can be traced back to accumulation of excessive nonlinear phase shift. Previous approaches to this problem were based on indirect reduction of effective nonlinearity. We consider direct management of nonlinearity in fiber lasers, which can be realistically considered with the demonstration that nonlinear phase shifts of either sign can be generated with femtosecond pulses.[1,2] Similar approaches in telecommunications were theoretically considered previously.[3,4]

Figure 1 is a schematic drawing of a soliton laser. Amplitude modulation (AM) produced by a real or an artificial saturable absorber (SA) is necessary for the initial formation of a solitonlike pulse and to stabilize the pulse against perturbations. We refer to an artificial SA if there is no real absorption; nonlinear transmittance is obtained through a nonlinear phase shift. An example of an artificial SA is nonlinear polarization evolution.[5] Gain fiber with self-focusing nonlinearity and anomalous dispersion can support solitons. Several gain materials are available for use at near-infrared frequencies; the most common are Er-, Yb-, and Nd-doped fibers. Among these, only Er-doped fiber benefits from the availability of anomalous dispersion in ordinary fiber.

The best reported results with Er fiber soliton lasers are several-hundred femtosecond pulses with energies of tens of picojoules. The most important obstacle to generation of shorter or higher-energy pulses or both is the perturbation that arises from variations of pulse energy over the cavity period that are due to loss (including output coupling) and gain. This perturbation manifests itself in the formation of discrete sidebands in the spectrum and is known as spectral sideband generation (SSG). A first-order treatment shows that the offset of the frequencies of the sidebands from the center of the spectrum is given by $\Delta\omega_n \sim \pm 1/\tau_p(8nz_s/z_c - 1)^{1/2}$, where n is the order of the sideband.[6,7] Here z_c is the cavity length, $z_s = \pi/2(\tau_p^2/\beta'')$ is the soliton period, β'' is the group velocity dispersion (GVD), and τ_p is the pulse width. It is experimentally found that z_c/z_s must be limited to <3 to prevent instability.[8] Thus SSG places a lower limit to pulse width. In the soliton regime, $E_p\tau_p = 2(\beta''/\gamma)$ (E_p is the pulse energy and γ is the Kerr nonlinearity), so this limitation becomes an upper boundary to pulse energy for a given fiber nonlinearity.

To achieve higher pulse energies or shorter pulses, two possibilities emerge: the use of a shorter cavity and reduction of the Kerr nonlinearity. There are limitations to a shorter cavity, one of which is imposed by the minimum length of fiber necessary for adequate gain. Additionally, a laser with a shorter cavity is more likely to be plagued by Q switching. Reduction of nonlinearity is therefore the preferable alternative for most situations. For femtosecond-pulse fiber lasers, nonlinearity reduction has been addressed most effectively by the stretched-pulse laser.[9] The stretched-pulse laser essentially implements dispersion management, which has been successful in optical communications.[10] As a result, SSG is suppressed.[11] Pulse stretching has resulted in the generation of 100-fs pulses of ~2.7-nJ energy.[12] In this approach, the effects of nonlinearity are reduced indirectly, through the effects of dispersion.

There are limitations to the stretched-pulse approach.

0740-3224/2002/030470-07$15.00 © 2002 Optical Society of America

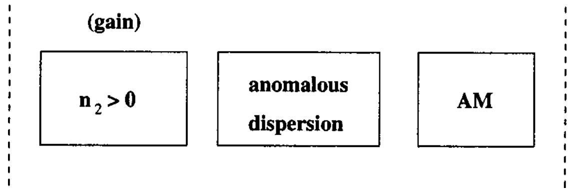

Fig. 1. Schematic of a generic soliton laser consisting of segments with self-focusing nonlinearity, anomalous dispersion, and amplitude modulation (AM).

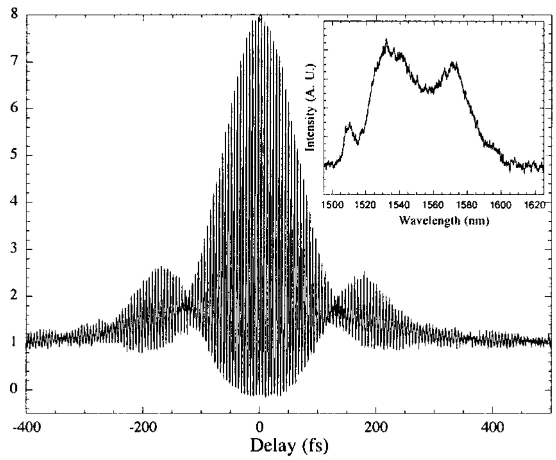

Fig. 2. Typical autocorrelation of the stretched-pulse laser in our laboratory. Inset, the corresponding spectrum.

Highly chirped, picosecond pulses are switched out of the laser, and these are compressed externally in a dispersive delay line. The need for an external compression stage is an inconvenience for applications. Although effective nonlinearity is reduced and higher energies are achieved, it is clear that the fundamental limitation imposed by excessive nonlinearity is not eliminated: This limitation manifests itself as a tendency to multiple pulsing as energy is increased. The stretching/compression ratio cannot be increased indefinitely without the appearance of undesirable effects on the pulse dynamics. Increasing the dispersion contrast by using higher-dispersion fiber in both sections of the dispersion map is limited by available fiber parameters, and it is clear that increasing the total positive dispersion will result in larger deviations from a linear chirp. Increased nonlinearity of the chirp limits compression and distorts the pulse shape. Typical interferometric autocorrelation and the corresponding spectrum produced by a stretched-pulse laser in our laboratory are shown in Fig. 2, and similar results were reported previously.[13] The structures in the spectrum and the time profile can be undesirable for many ultrafast applications as well as for amplification. Furthermore, dispersion management is possible only for Er-doped fiber near ~1.55 μm. Fiber lasers are needed at shorter wavelengths, where only normal dispersion is available. Novel microstructured fiber may provide anomalous dispersion. However, because of their small effective areas, these fibers have increased nonlinear effects, which would be a limitation on high-energy pulse generation.

In this paper we propose direct management of nonlinearity by use of negative (self-defocusing) nonlinear phase shifts. In Section 2 we describe the concept of a fiber laser that is essentially free of spectral sidebands. Elimination of sidebands is achieved by use of dispersion and nonlinearities of both signs. In Section 3 we consider the use of negative nonlinearities without optimizing dispersion. This is a less desirable scheme but one that will be easier to implement. In Section 4 we discuss practical implementation of nonlinearity management in fiber lasers. Section 5 summarizes our main conclusions.

2. NONLINEARITY- AND DISPERSION-MANAGED SOLITONS

The use of negative nonlinearities is a degree of freedom that to our knowledge was not previously explored in the design of short-pulse fiber lasers. Let us consider a general dispersion and nonlinearity map described by the nonlinear Schrödinger equation written in normalized units:

$$\frac{\mathrm{d}u}{\mathrm{d}z} - i\frac{1}{2}D(z)\frac{\mathrm{d}^2u}{\mathrm{d}t^2} = i\Gamma(z)|u|^2u, \tag{1}$$

where $D(z)$ and $\Gamma(z)$ can take the values -1 to $+1$ across the map. Although one can consider arbitrary variations, in practice it is realistic to consider only piecewise constant maps composed of a small number of segments. In particular, we shall consider the following simple map:

$$D(z) = \Gamma(z) = \begin{cases} +1 & 0 < z < \xi z_c \\ -1 & \xi z_c < z < z_c \end{cases},$$

where ξ:$0 < \xi < 1$ and determines the relative strength of the two segments. The conceptual model of a laser based on this map is illustrated in Fig. 3. Both segments support formation of a soliton with identical parameters. However, the signs of the dispersion and nonlinearity operators are reversed. Hence it is expected that the solution for the fundamental soliton will become

$$u = \mathrm{sech}(t)\exp[i\delta(z)/2], \tag{2}$$

where $\delta(z) = D(z) = \Gamma(z)$. For the special case of $\xi = 1/2$, the effects of each segment are exactly compensated for by the following segment. Indeed, any input field is an eigensolution. We call this scheme full compensation.

In a real system the implementation cannot be ideal, and there will be departures from full compensation. An equally attractive approach is to implement the map such that $\xi \neq 1/2$, which we denote partial compensation. In this case the map has a reduced effective length, defined

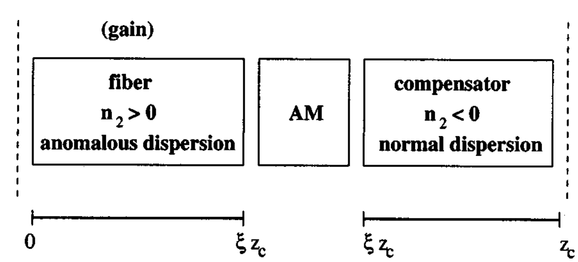

Fig. 3. Block diagram of the proposed laser consisting of fiber, compensator, and SA. We envisage a ring cavity for increased ease of self-starting. The sequence of the components in the diagram is the same as in the simulations.

as $z_{c,\mathrm{eff}} = |2\xi - 1|z_c$. The phase shift accumulated by the soliton will be proportional to the difference of normalized lengths of the two segments, as opposed to the total length. That this is so has important consequences for SSG: The sidebands are expected to move toward larger frequency offsets from the center of the spectrum. Adapting a simple model of SSG similar to that of Ref. 6, we introduce lumped loss (e.g., output coupling) at the end of the map, balanced by linear gain throughout the map:

$$\frac{\mathrm{d}u}{\mathrm{d}z} - i\frac{1}{2}D(z)\frac{\mathrm{d}^2u}{\mathrm{d}t^2} = i\Gamma(z)|u|^2u + gu, \tag{3}$$

where $D(z)$ and $\Gamma(z)$ are defined as before. The lumped loss at the end of the second segment is described by $u \to u\exp(-gz_c)$. With the transformation $u \to A(z)u$, it can be shown that the energy variation that is due to loss and gain is equivalent to a variation in the effective nonlinearity experienced by the soliton, with $A(z)$ characterizing this variation. With simple algebraic manipulation, Eq. (3) takes the form

$$m(z)\frac{\mathrm{d}u}{\mathrm{d}z} - i\frac{1}{2}\frac{\mathrm{d}^2u}{\mathrm{d}t^2} = iA^2(z)|u|^2u, \tag{4}$$

where $m(z) = -1/D(z) = -1/\Gamma(z)$. Using the scaling properties of a nonlinear Schrödinger equation, we can express the nonperturbed solution as

$$u = \eta\,\mathrm{sech}[\eta(t - wz)]\exp[i\delta(z)(wt - kz)], \tag{5}$$

where $k = (\omega^2 - \eta^2)/2$. We look for a solution of this form for Eq. (4) and replace $A^2(z)$ with its Fourier series expansion. A first-order expansion for small perturbations shows that resonances occur for $\int_0^{z_c} k\,\delta(z)\mathrm{d}z = 2\pi n$. The integral equals the difference between the total phase accumulated by the perturbed soliton and the dispersive waves and is proportional to the effective map length, $z_{c,\mathrm{eff}}$. Hence the frequencies at which the sidebands are formed become a function of a (smaller) effective map length, not of the total map length. The sideband frequency offsets are given by

$$\Delta w_n \sim \pm 1/\tau_p[8nz_s/(z_c|2\xi - 1|) - 1]^{1/2}. \tag{6}$$

The sidebands can be pushed out to large offsets, where there is little energy, by choice of ξ close to 1/2. Thus SSG is effectively suppressed; this is the main result of this section.

We used numerical simulations to evaluate this concept in detail. Because we envisage the application of these ideas to femtosecond fiber lasers, we made the simulations by assuming a fiber laser based on the proposed map. We consider a ring laser design for increased ease of self-starting. The first segment consists of gain fiber with finite gain bandwidth. The compensating segment has normal dispersion and self-defocusing nonlinearity, and it is labeled the compensator. To illustrate the concept, we used normalized units in the simulations. Implementation with realistic parameters is discussed later in the text. The length of the compensator $[(1 - \xi)z_c]$ was increased, starting from zero, while the fiber was shortened such that the total cavity length was kept constant at $z_c = 10$. For every simulation, a control simulation was run that corresponded to a laser consisting only of gain fiber with a physical length equal to $z_{c,\mathrm{eff}}$. The dispersion and nonlinearity of the fiber and the compensator were chosen to yield the characteristic dispersion and nonlinear lengths $L_D = \tau_p^2/\beta'' = 1$ and $L_{\mathrm{NL}} = 1/(\gamma P_p) = 1$ (P_p is the peak power). Gain is modeled as distributed over the length of the fiber and saturating with total intracavity energy (E) with a Gaussian frequency dependence: $g(E, \omega) = g_0(1 - E/E_{\mathrm{sat}})\exp[-(\omega - \omega_0)^2/\Omega_{bw}^2]$. Here E_{sat} is the gain saturation energy, ω_0 is the carrier frequency and Ω_{bw} is the gain bandwidth. Small-signal gain is approximately 30 dB, and E_{sat} is set to the energy of a fundamental soliton in normalized units. If the normalized pulse duration is assumed to be 100 fs in physical units, the gain bandwidth corresponds to ~50 nm. The SA and the output coupling (linear loss, in general) are modeled as a transmission function of the form $u \to u\,[(1 - \alpha - \beta) + \alpha\sin^2(\pi I/I_{\mathrm{sat}})]$. Here I denotes the instantaneous intensity and I_{sat} is the saturation intensity, which is set to the peak intensity of the soliton unless stated otherwise. $\beta = 10\%$ is the output coupling, and $\alpha = 10\%$ is the modulation depth. Thus the round-trip loss of the laser for cw light is 20%. We note that the exact value of linear loss is not crucial if the gain is strong enough, because the nonlinearity of the subsequent segment can be set to offset a decrease in energy.

We begin by considering partial compensation for varying $z_{c,\mathrm{eff}}$. All the simulated cases resulted in self-starting stable solitary pulses (the buildup of the pulse from noise for $z_{c,\mathrm{eff}} = 1$ is illustrated in Fig. 4). The departure of the sidebands from the center of the spectrum with increasing compensation ratio is illustrated in Fig. 5(a), and the offset of the first sidebands relative to control simulations is plotted in Fig. 5(b). For the highest compensation that was simulated ($z_{c,\mathrm{eff}} = 0.1$), the pulse energy is increased by a factor of 100 in the proposed scheme, whereas the offset of the first sideband is equivalent to that in the uncompensated soliton laser.

For full compensation (corresponding to vanishing $z_{c,\mathrm{eff}}$), the enhancement in energy is smaller than for $z_{c,\mathrm{eff}} = 0.1$. Spectral sidebands are eliminated at ener-

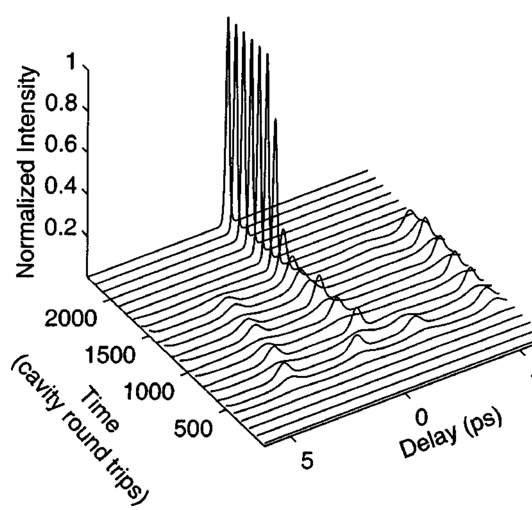

Fig. 4. Buildup of a solitary pulse from intracavity noise plotted for the proposed laser with $z_{c,\mathrm{eff}} = 1$.

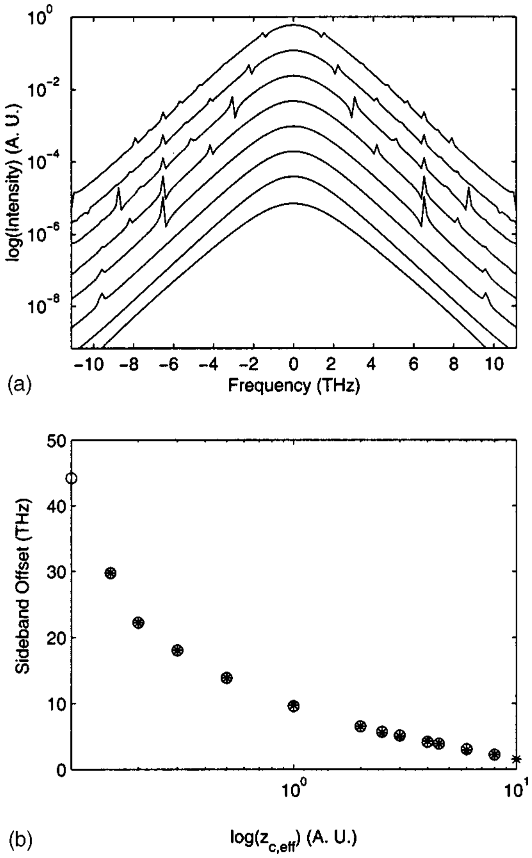

Fig. 5. (a) Spectra (as offset from the carrier frequency) for effective map lengths of (top to bottom) $z_{c,\text{eff}} = 10, 8, 6, 4, 2, 1, 0.5, 0.1$. (b) Plot of the frequency offset of the first sidebands for the proposed laser and the control simulation.

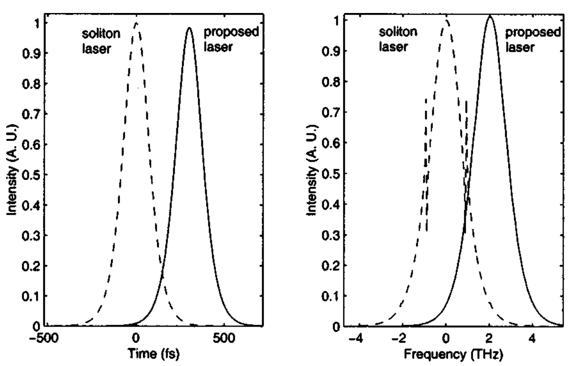

Fig. 6. Results of simulations for full compensation ($\xi = 1/2$): SSG is eliminated, and similar pulse duration is achieved at 10 times higher energy than in the soliton laser. The traces have been displaced horizontally for clarity.

gies that are an order of magnitude higher than for the ordinary soliton laser. The proposed laser produces pulses with a time profile virtually indistinguishable from that of the soliton laser with 10 times higher pulse energy (Fig. 6). The energy can be increased to larger values. However, deviations from ideal compensation caused by noninstantaneous recovery of the loss begin to distort the pulse. Full compensation, however, has a remarkable feature. It constitutes a mode-locking mechanism that is dominated not by soliton effects but by the SA: The peak intensity of the pulse is determined by the saturation intensity of the SA. The reduced influence of solitary effects explains the result mentioned above, namely, that full compensation does not scale to energies as high as for partial compensation. If the saturation intensity of the SA is set to a value that does not correspond to the fundamental soliton (intracavity energy is constant), breathing pulses result. If the gain bandwidth is much larger than the pulse bandwidth, the peak intensity of the pulse increases linearly with the saturation intensity of the SA. This linear increase saturates as the pulse bandwidth becomes comparable with the gain bandwidth.

The consequences of an ideal compensation of the effects of the fiber are obvious from an elementary consideration of the nonlinear Schrödinger equation. The benefits that we expect from this approach, however, pertain to reduction of the effects of perturbations. In the presence of perturbations the compensation is inherently not ideal. Thus it was not clear *a priori* that these expectations would prevail in a real fiber laser. We see from numerical simulations that self-starting solitary-pulse formation at high energies is possible.

To summarize the substantial benefits of this approach:

(1) The idealized system with full compensation is essentially independent of pulse shape and energy. As a consequence of this, SSG is not present, even for higher-power fiber lasers, and SA dominates pulse dynamics.

(2) For a more realistic implementation, we consider partial compensation. Compensation such that $z_{c,\text{eff}} < 1$ practically eliminates SSG.

3. NONLINEARITY MANAGEMENT WITHOUT DISPERSION OPTIMIZATION

The use of nonlinearity and dispersion of either sign is a promising avenue to creating a fiber–compensator pair. However, it may not be possible or practical to achieve the desired parameters, in particular, sufficient dispersion of correct sign for the negative-nonlinearity segment, for many applications. In this section we briefly consider other approaches to nonlinearity management that are less than ideal but that can provide significant advantages.

It will be difficult to compensate for the GVD of more than several meters of fiber. It is, however, possible to produce large negative nonlinear phase shifts. This fact leads us to consider nonlinearity management without fine control of dispersion. Reduction of average nonlinearity should permit formation of higher-energy pulses.

We performed numerical simulations to investigate this expectation. A soliton fiber laser was chosen rather than a stretched-pulse laser because it is better understood quantitatively. The simulated laser is depicted schematically in Fig. 7. The model used in the simulations is the same as described in Section 3. However, the compensating segment provides only negative nonlinear phase shifts, and it has negligible dispersion. A simulation without the compensating segment serves as the baseline. The gain saturation energy was increased to two, three, and four times that of a fundamental soliton. The magnitude of the compensating nonlinearity was in-

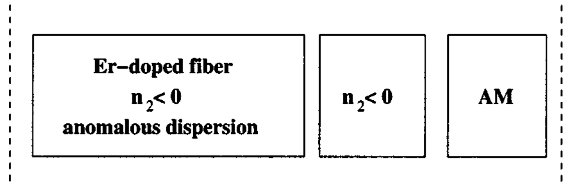

Fig. 7. Schematic of a fiber laser with reduced average nonlinearity.

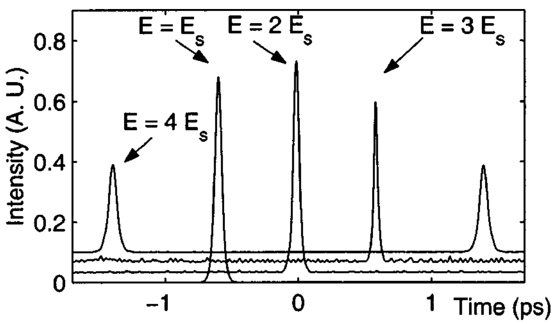

Fig. 8. Results of numerical simulations of a soliton fiber laser, showing the intensity profiles with increasing pulse energy and nonlinearity compensation. The intensity profiles are normalized and have been displaced vertically and horizontally for clarity.

creased accordingly, such that the increase in pulse energy was balanced by the decrease in the average nonlinearity. The intensity profiles of the resultant pulses are shown in Fig. 8. We can increase the energy by a factor of 2 by decreasing the average nonlinearity. However, for a threefold increase, the resulting pulse sheds radiation, which is visible as small intensity fluctuations away from the pulse. When the energy is increased to four times the original value, the pulse breaks into two, resulting in irregular double-pulsing.

The order in which nonlinearity and dispersion act on the pulse matters. From a physical point of view, this limitation means that the pulse in the first segment should not be severely distorted before it reaches the compensating segment. From the numerous simulations performed we see that, as a rule of thumb, a total nonlinear phase shift of $\sim\pi$ is the maximum that can be compensated for without dispersion optimization. Further increases in energy can be achieved without pulse breakup and multiple-pulse formation by the introduction of additional compensating segments at equidistant positions in the cavity. Unfortunately, the benefits of such an approach will be proportional to the number of compensating segments used. The use of more than two compensating segments seems impractical. In summary, the addition of compensating materials promises a reduction of average nonlinearity for soliton and DM fiber lasers, but, in practice, improvement appears to be limited to a severalfold increase in pulse energy.

As another example of nonlinearity management, we briefly consider the use of negative nonlinearities for the design of fiber lasers at $\lambda < 1.3\ \mu$m. An all-fiber, high-energy femtosecond laser in the 1.0–1.3-μm region is highly desirable for applications such as medical imaging. However, at these wavelengths, ordinary fiber has normal dispersion. Anomalous dispersion can be obtained with prism pairs or diffraction gratings, but these offset the primary advantages of fiber lasers. Microstructured fibers offer anomalous dispersion through the use of large waveguide dispersion to offset the material dispersion and may be useful for soliton pulse shaping. An alternative approach is to form solitons with $n_2 < 0$ and positive GVD. This approach has already been demonstrated experimentally for a bulk solid-state laser.[1] Numerical simulations that use existing material properties show that generation of 100-fs pulses with more than 100-pJ energy is feasible with this approach.

In conclusion, reduction of average nonlinearity offers limited but significant improvement in pulse energy compared with existing soliton and stretched-pulse lasers and is considerably easier to implement than the fiber-compensator pair. We have considered the addition of one segment with $n_2 < 0$ of negligible dispersion. It is likely that one can achieve better results through optimization of the map by the use of more than one type of fiber and careful consideration of the ordering of the segments.

4. IMPLEMENTATION OF NONLINEARITY MANAGEMENT

The experimental implementation of nonlinearity management relies on the presence of suitable materials with negative (self-defocusing) Kerr nonlinearity. Semiconductors have large self-defocusing refractive nonlinearity ($\sim$1000 times that of fused silica) for $h\nu > 0.7\ E_{\text{bandgap}}$. However, the negative nonlinearity is associated with strong two-photon absorption, which is a nonlinear loss. Large two-photon absorption becomes detrimental for short-pulse formation at rather low intensities because the modulation depth of the SA is limited. Thus these materials are unattractive for high-energy fiber laser design. An alternative to semiconductors is the effective negative nonlinearity produced by cascaded quadratic processes.[14] Liu and co-workers have shown that $\Delta\Phi^{\text{NL}} \sim \pi$ can be impressed on femtosecond pulses with small ($<$1%) loss to second-harmonic generation by use of the cascade processes at large phase mismatch.[1,2]

Consider the construction of a fiber laser based on this concept, with Er-doped fiber as the gain medium for $\sim$1550 nm. Fiber with anomalous dispersion of several square picoseconds per kilometer and small third-order dispersion is available. Any of several crystals can be used as the quadratic medium. In particular, periodically poled lithium niobate (PPLN) in waveguide geometry shows promise.[15] The dispersion of PPLN for type I phase matching is $\sim$100 ps^2/km at 1550 nm. Thus the dispersion of 1-m-long gain fiber can be compensated for with a PPLN waveguide a few centimeters in length. With a 70-mm-long waveguide, we estimate that the nonlinear phase accumulation of a fiber $\sim$10 m in length can be compensated for at ΔkL large enough to avoid the detrimental effects of group-velocity mismatch for 100-fs pulses. Thus dispersion, rather than nonlinearity, will be the limiting factor in the construction of a compensator. Similarly, for the construction of a soliton-supporting Nd- or Yb-doped fiber laser at $\sim$1 μm, the use of cascaded processes in a PPLN waveguide appears to

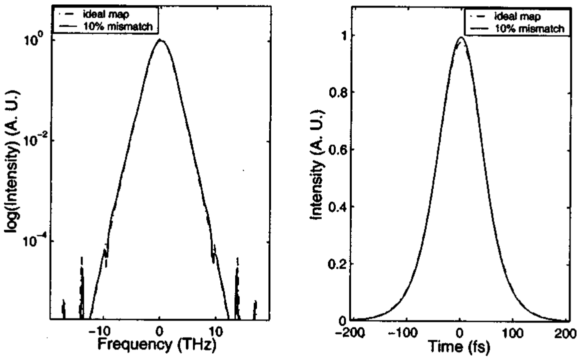

Fig. 9. Intensity profile and spectrum (as offset from the carrier frequency) of the proposed laser with $z_{c,\text{eff}} = 0.1$ compared with the same laser with 10% mismatch in the nonlinearity coefficient of the compensating segment.

hold promise. According to our calculations, it should be possible to balance the nonlinearity of gain fiber ~10 m in length at the phase mismatches necessary to support ~100-fs pulses. It is clear that implementation of the approaches considered here will require the solution of challenging material problems. Nevertheless, we see that it is possible to form a compensator by means of cascaded processes in existing and available materials.

A fast SA is necessary for femtosecond pulse formation. Nonlinear polarization evolution (NPE) or the use of a nonlinear optical loop mirror requires the use of fiber at least several meters long to accumulate the nonlinear phase needed for sufficient modulation depth. This requirement imposes a challenging minimum length of fiber to be compensated for. Additionally, because of the interferometric nature of these techniques, there is a maximum energy for a given pulse shape beyond which loss increases with increasing pulse energy. This effect is referred to as the saturation of NPE. For this purpose, NPE produced by the use of cascaded quadratic nonlinearities[16] should be advantageous, because it can be implemented in a several-centimeter-long frequency-doubling crystal. Saturation of NPE can be prevented because the saturation energy can be set to high values through the choice of phase-mismatch and crystal parameters. NPE works equally well with negative or positive nonlinear phase shifts. Therefore it may be possible to accomplish AM in the compensator itself.

In a real implementation, in addition to problems caused by the perturbations on the pulse that are inherent in the operation of a pulsed laser, there may be difficulties in precise matching of the fiber and the compensator. We tested the robustness of the proposed laser by intentionally mismatching the parameters in the numerical simulations. Mismatches of 10% in either parameter are easily tolerated, even for a high degree of compensation (corresponding to $z_{c,\text{eff}} = 1$; Fig. 9). The resultant pulse shape does not change appreciably, and the sideband frequency offset from the center of the spectrum decreases by only a few percent. Finally, we note that it is possible to consider hybrid approaches for which the average dispersion of the fiber section is decreased by the use of dispersion-compensating fiber, as in dispersion-managed systems. A potential advantage of such an approach is that the need to obtain sufficient dispersion in the compensator is likely to be a greater limitation than nonlinearity. As long as the combined effect of the two fibers is a good approximation of a single fiber of uniform dispersion equal to their average dispersion, the degradation in the laser operation will be small. In summary, despite the difficulties that need to be confronted for a practical application of nonlinearity management, we can see that existing materials already have properties that offer some promise of suitability for nonlinearity management.

5. CONCLUSION

In conclusion, we propose the use of negative nonlinearity as a new degree of freedom in the design of short-pulse fiber lasers. We describe a nonlinearity- and dispersion-managed map and demonstrate that it is essentially free of spectral sideband generation. This approach permits the pulse energy in a soliton fiber laser to be increased by 2 orders of magnitude. Implementation by the use of existing materials appears to be feasible but challenging. As another application of nonlinearity management, we consider the less than ideal but easier to implement approach of reducing average Kerr nonlinearity by the inclusion of a negative nonlinearity segment into the cavity. This approach offers significant benefits but is limited because of noncommutation of self-phase modulation and GVD. Studies are in progress for experimental implementation. Although we focus on applications to high-energy or shorter pulse formation from fiber lasers, the concept is general and applies to passive propagation of short pulses in optical fiber. Consequently, nonlinearity management is likely to be useful in soliton communications as a way to prevent spectral sidebands and excessive nonlinear phase shifts.

ACKNOWLEDGMENTS

This research was supported by the National Institutes of Health under grant RR10075. The authors thank Clark-MXR, Inc., for equipment and Matthew Bolcar for help with numerical simulations.

F. Ö. Ilday's e-mail address is ilday@cornell.edu.

REFERENCES

1. L. J. Qian, X. Liu, and F. W. Wise, “Femtosecond Kerr-lens mode locking with negative nonlinear phase shifts,” Opt. Lett. **24**, 166–168 (1999).
2. X. Liu, L. Qian, and F. W. Wise, “High-energy pulse compression using negative phase shifts produced by the cascade $\chi^{(2)}:\chi^{(2)}$ nonlinearity,” Opt. Lett. **24**, 1777–1779 (1999).
3. C. Pare, A. Villeneuve, and P.-A. Belanger, “Compensating for dispersion and the nonlinear Kerr effect without phase conjugation,” Opt. Lett. **21**, 459–461 (1996).
4. C. Pare, A. Villeneuve, and S. LaRochelle, “Split compensation of dispersion and self-phase modulation in optical communication systems,” Opt. Commun. **160**, 130–138 (1999).
5. M. Hofer, M. E. Fermann, F. Haberl, M. H. Ober, and A. J. Schmidt, “Mode locking with cross-phase and self-phase modulation,” Opt. Lett. **16**, 502–504 (1991).
6. S. M. J. Kelly, “Characteristic side-band instability of periodically amplified average soliton,” Electron. Lett. **28**, 806–807 (1992).

7. B. A. Malomed, "Propagation of a soliton in a nonlinear waveguide with dissipation and pumping," Opt. Commun. **61**, 192–194 (1987).
8. K. Tamura, C. R. Doerr, H. A. Haus, and E. P. Ippen, "Soliton fiber ring laser stabilization and tuning with a broad intracavity filter," IEEE Photonics Technol. Lett. **6**, 697–699 (1994).
9. K. Tamura, E. P. Ippen, H. A. Haus, and L. E. Nelson, "77-fs pulse generation from a stretched-pulse mode-locked all-fiber ring laser," Opt. Lett. **18**, 1080–1082 (1993).
10. N. J. Smith, N. J. Doran, W. Forysiak, and F. M. Knox, "Soliton transmission using periodic dispersion compensation," J. Lightwave Technol. **15**, 1808–1822 (1997), and references therein.
11. D. J. Jones, Y. Chen, H. A. Haus, and E. P. Ippen, "Resonant sideband generation in stretched-pulse fiber lasers," Opt. Lett. **23**, 1535–1537 (1998).
12. G. Lenz, K. Tamura, H. A. Haus, and E. P. Ippen, "All-solid state femtosecond source at 1.55 μm," Opt. Lett. **20**, 1289–1291 (1995).
13. L. E. Nelson, S. B. Fleischer, G. Lenz, and E. P. Ippen, "Efficient frequency doubling of a femtosecond fiber laser," Opt. Lett. **21**, 1759–1761 (1996).
14. R. DeSalvo, D. J. Hagan, M. Sheik-Bahae, G. Stegeman, E. W. Van Stryland, and H. Vanherzeele, "Self-focusing and self-defocusing by cascaded second-order effects in KTP," Opt. Lett. **17**, 28–30 (1992).
15. R. Schiek, M. L. Sundheimer, D. Y. Kim, Y. Baek, G. I. Stegeman, H. Seibert, and W. Sohler, "Direct measurement of cascaded nonlinearity in lithium niobate channel waveguides," Opt. Lett. **19**, 1949–1951 (1994).
16. X. Liu, F. Ö. Ilday, K. Beckwitt, and F. W. Wise, "Femtosecond nonlinear polarization evolution based on cascade quadratic nonlinearities," Opt. Lett. **25**, 1394–1396 (2000).